Purdue University

Purdue e-Pubs

Department of Electrical and Computer Engineering Technical Reports

Department of Electrical and Computer Engineering

3-1-1988

Coordinated Motion Control of Multiple Robotic Devices for Welding and Redundancy Coordination through Constrained Optimization in Cartesian Space

Shaheen Ahmad
Purdue University

Shengwu Luo
Purdue University

Coordinated Motion Control of Multiple Robotic Devices for Welding and Redundancy Coordination through Constrained Optimization in Cartesian Space
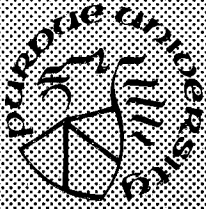
Shaheen Ahmad
Shengwu Luo

TR-EE 88-14
March 1988

School of Electrical Engineering
Purdue University
West Lafayette, Indiana 47907

Coordinated Motion Control of Multiple Robotic Devices for Welding[**]

and

Redundancy Coordination through Constrained Optimization in Cartesian Space

Shaheen Ahmad, Shengwu Luo

Real-time Robot Control Laboratory

School of Electrical Engineering

Purdue University

West Lafayette, Indiana 47907

USA

Abstract

In this paper we consider the problem of coordinating multiple motion devices for welding. We focus on the problem of coordinating a positioning table and a seven axis manipulator, given the parametric definition of a trajectory on a weld piece. The problem is complex as there are more than nine axis involved and a number of permutations are possible which achieve the same motions of the weld torch. The system is

redundant and the robot has singular configurations. As a result, manual programming of the robot system is rather complex.

Our approach to the coordination problem is based on subdivision of constraints. The welding table is coordinated to ensure down-handed welding convention, while the seven axis robot (a six axis Cybotech WV15 robot and track) are coordinated to track the weld point. The coordination is achieved by keeping the robot in good maneuverability position, so as to avoid the robots singularity conditions and motion limits of the track. We were able to express the singularity conditions in terms of cartesian coordinates [1]. As a result, we could obtain analytic solution to our optimization of the maneuversability and therefore avoid using known pseudoinverse techniques which are known to exhibit inaccuracies [2]. The output of our optimization process is the positions of the track and the robot end-effector, these positions are used to generate the joint angles of the arm by inverse kinematics.

Introduction

In this paper we address the problem of coordinating a two axis table and a seven axis robot, given the mathematical description of the weld seam trajectory with reference to the part coordinate frame. The welding is to be carried out in down-handed convention to allow the plasma to flow appropriately along the weld contour. This requires the weld piece surface normal to be aligned in the opposite direction of the gravity vector throughout the entire welding process. A seven axis robot consisting of a track and a six-axis arm is used to guide the weld torch. Redundant manipulator systems are quite often used in welding systems because, (i) a larger robot work envelope is obtained, (ii) singular configurations in the robot can be avoided by optimal movement of the redundant axes, i.e. the track.

The part positioning table is used to manipulate the part into a position and orientation which is best suited for the given task constraints. The manipulator is then required to produce the desired torch motion to achieve the weld. Manual programming of the robot welding system is complex and several iteration may be required before a suitable program is taught which successfully coordinates both the positioner and the robot. A mathematical process which generates the movement of the redundant robot and the welding table without using pseudo-inverse techniques is described in this paper.

Recently, there has been growing interest in the research community investigating the problem of coordinated motion control of non-redundant multiple robotic devices and the progress in this field has been rapid [10], [3], [26]. Our work is more closely related to coordinating redundant manipulators. Past research in the area of redundancy coordination has involved the resolved motion rate technique [12], using the pseudo-inverse of the Jacobian matrix [5], [4], [9], [12], [17], [21], [22]. In the resolved motion rate method, $\underset{\sim}{\dot{\theta}}$ is used to guide the manipulator. The (n×1) joint velocity vector $\underset{\sim}{\dot{\theta}}$ is related to the (m×1) end effector velocity vector as:

$$\underset{\sim}{\dot{x}} = J \underset{\sim}{\dot{\theta}} \tag{1}$$

where J is the non square (m×n) manipulator Jacobian, and as n > m, usually m = 6 for six degrees of freedom, then general solution for $\underset{\sim}{\dot{\theta}}$ is:

$$\underset{\sim}{\dot{\theta}} = J^+ \underset{\sim}{\dot{x}} + (I - J^+J) \underset{\sim}{u} \tag{2}$$

where I is a (n×n) unit vector and $\underset{\sim}{u}$ is an (n×1) arbitrary vector, J^+ is the pseudo-inverse of the jacobian, which is defined as:

$$J^+ = J^T(JJ^T)^{-1} \tag{3}$$

The term $(I - J^+J)$ is the null space of J. In order to avoid singular configuration.

Yoshikawa [9] suggested the selection of $\underset{\sim}{u}$ such that the scalar ν is maximized, where

$$\nu = \sqrt{\det(\mathbf{JJ^T})} \tag{4}$$

Thus we may select, $\underset{\sim}{u} = \underset{\sim}{\nabla}\nu$. Once $\underset{\sim}{\theta}^{\cdot}$ is found, $\underset{\sim}{\theta}$ (t) is accumulated as:

$$\underset{\sim}{\theta}(t) = \int_{t_0}^{t} \underset{\sim}{\theta}^{\cdot} \, dt + \underset{\sim}{\theta}(t_0) \tag{5}$$

Several computational difficulties arise here, if m $=$ 6 and n $\geqq$ 7, *it may be difficult to find* the Jacobian **J** in symbolic form (in terms of θ), in which case numerical calculation of **J** is necessary. The pseudo-inverse of **J**, $\mathbf{J^+}$ must be numerically computed, as symbolic forms of $\mathbf{J^+}$ (for n $\geqq$ 7) is not easily obtained. Once **J**, $\mathbf{J^+}$ and $\underset{\sim}{u}$ is calculated based *on the previous value of the joint angle*, $\underset{\sim}{\theta}^{\cdot}$ is calculated and the joint angle $\underset{\sim}{\theta}$ (t) is obtained by integration.

In addition to the large amount of computational steps which are needed for the numerical calculation, Chang [2] notes several other defiencies [2]: (i) Inaccurate joint solutions, due to the linear approximations made when evaluating Equation (2) for the joint rate. (ii) Errors in accumulating $\underset{\sim}{\theta}$ (t) from joint rates $\underset{\sim}{\theta}^{\cdot}$. This is a minor point. (iii) Problems with repeatability of motion as the vector $\underset{\sim}{u}$ is sensitive to the direction of approach.

Chang [2] derived a closed-form solution to remedy the above problems, however, the computational issue remained and numerical algorithms have to be used to solve for the joint angles. Extended Jacobian method [1] is also computationally intensive and is only applicable to systems with one degree of redundancy.

The redundancy coordination scheme proposed in this paper is based on constrained optimization of an objective function in cartesian coordinates. A redundant manipulator with less than 13 degrees of freedom, but greater than or equal to seven

degrees of freedom may be regarded as two non-redundant manipulators. Each manipulator with explicit inverse kinematic solutions. As we are able to express singularity condition [1] in cartesian coordinates of the end effectors, we are also able to setup a constraint function in cartesian coordinates. Then the coordination task can be posed as an optimization problem, so as to maintain the redundant arm on a desired trajectory while avoiding the activation of the singularity constraints, and simultaneously minimizing the objective function. The optimization can be expressed in terms of the end effector coordinates of the first (nonredundant sub-manipulator) manipulator and the desired trajectory. The optimization is used to find the position of the first manipulator. The position of the second (the redundant sub-manipulator) end-effector can then be found by direct kinematic (see later).

The first section of this paper describes our solution methodology, the second section presents the necessary mathematics to model the weld contour and to solve for the inverse kinematics of the part positioning table. The kinematics of the robot and its singularity states are discussed in section three. The proposed method of singularity avoidance and the coordination of the redundant joints through constrained minimization is discussed in section four. A simulation of a welding operation with a redundant manipulator is presented in section five to verify the proposed methodology. Conclusion of the paper is presented in section six.

I. Subdivision of the Coordination Problem

The multiple-device coordination problem can be solved by dividing the problem into small subtasks. The solution of the subtasks are required to satisfy the following global and local constraints.

(a)   The surface normal of the weld part has to be anti-parallel to the direction of gravity. The positioning table must be coordinated so as to achieve this.

(b)   The inverse kinematics of the six degree of freedom manipulator is used to generate the motion of the weld torch.

(c)   The extra degrees of freedom present in the manipulator is used to keep the robot out of singular configurations or to increase its reach.

A block diagram representing the hierarchial coordination of the devices is shown in Figure 1. The processing stages in each block forms the basis of our task subdivision:

(i)   The data from the CAD station is used to generate the path the weld tip must trace.

(ii)   This information is utilized by the coordinator to generate table movement subject to constraints (a) in the above.

(iii)   Next, the joint angles of the table are calculated. Differential approximations are not used to generate the joint angles.

(iv)   The motion of redundant system is generated through a nonlinear optimization process, such that singularity conditions are avoided and robot reach is optimized.

(v)   The joint angles of the WV15 robot and the position of the track are next computed using exact inverse kinematics solutions.

<div align="center">

II. Geometric Model of the Weld Contour

and the Positioning Table

</div>

Figure 2 indicates the relative location of the positioning table and the part with respect to a reference frame **O** (world origin frame). The following transforms are defined:

$^{O}\mathbf{Torg}$ = origin of the positioning table with respect to the reference frame O.

$^{Torg}\mathbf{Tbl}$ = center of the positioning table with respect to the table reference frame.

$^{\text{Tbl}}$**Part** = location of the weld parts reference frame with respect to the table center.

$^{\text{Part}}$**Sur** = a weld point defined on the surface of the part, with respect to reference frame **Part**.

θ_1, θ_2, θ_3 = tables joint variables, in this case θ_1 is fixed.

Geometric Description of Weld Part

We adopt cylindrical coordinates $(r, \alpha, z)^t$ to describe the position of the weld contour on the surface of the part, with respect to a part reference frame. We assume the shape of the part is arbitrary, but it may be described by Equation (7). If $^{\text{Part}}\underline{P}_{\text{sur}}$ is a vector which is located on the weld contour it is defined as:

$$^{\text{Part}}\underline{P}_{\text{sur}} = (r\cos\alpha, \ r\sin\alpha, \ z)^t \tag{6}$$

where r, α and z are subject to a surface equation of the part

$$\text{surf}(r, \alpha, z) = 0 \tag{7}$$

Let $\underline{a}_{\text{sur}}$ be the direction of the surface normal, and $\underline{o}_{\text{sur}}$ be the direction of the surface tangent aligned along the weld contour. The normal of the surface $\underline{a}_{\text{sur}}$ is then given as:

$$\underset{\sim}{a}_{\text{sur}} = \frac{1}{a_0} \left[\frac{\partial z}{\partial r} r\cos\alpha - \frac{\partial z}{\partial \alpha} \sin\alpha, \ \frac{\partial z}{\partial r} r\sin\alpha + \frac{\partial z}{\partial \alpha} \cos\alpha, \ -r \right]^t \tag{8}$$

Here the normalization constant a_0 is defined as: $a_0 = \left\{ \left(\frac{\partial z}{\partial r} r\cos\alpha - \frac{\partial z}{\partial \alpha} \sin\alpha \right)^2 \right.$

$\left. + \left(\frac{\partial z}{\partial r} r\sin\alpha + \frac{\partial z}{\partial \alpha} \cos\alpha \right)^2 + r^2 \right\}^{1/2}$ Then, a weld trajectory on the part can be described parametrically by the below functions:

$$z = zcv(t)$$
$$\alpha = \alpha cv(t) \tag{9}$$
$$r = rcv(t)$$

where t is the variable denoting time. The tangent to this curve $\underset{\sim}{O}_{sur}$ is given as:

$$\underset{\sim}{O}_{sur} = \frac{1}{b_o} \left[\frac{d}{dt}(rcv(t).\cos(\alpha cv(t))), \ \frac{d}{dt}(rcv(t).\sin(\alpha cv(t))), \ \frac{d}{dt}(zcv(t)) \right]^t \tag{10}$$

where,

$$b_o = + \left\{ \left[\frac{d}{dt} zcv(t) \right]^2 + \left[\frac{d}{dt}(rcv(t).\cos(\alpha cv(t))) \right]^2 + \left[\frac{d}{dt}(rcv(t).\sin(\alpha cv(t))) \right]^2 \right\}^{1/2} \tag{11}$$

The normal vector $\underline{n}_{sur}$ can be found from $\underset{\sim}{n}_{sur} = \underset{\sim}{O}_{sur} \times \underset{\sim}{a}_{sur} = [n_x, \ n_y, \ n_z]^t$

Weaving Motions About the Weld Trajectory

In order to get an even weld fill, a small sinusoidal motion is superimposed on the nominal weld trajectory. The weaving motion in the sur reference frame can be described as a deviation of the torch at right angles to the specified weld path such that it is on the weld surface. The amplitude of the deviation is:

$$x_w = \delta_w \sin\left(\frac{2\pi V_p t}{l_w}\right) \tag{12}$$

where V_p is the weld path speed, δ_w is the weave amplitude, l_w is the weave wavelength

Therefore the weld trajectory points are slightly altered:

$$^{Part}\underline{P}_{weld} = {}^{Part}\underline{P}_{sur} + \left[\underline{n}_{sur}, \underline{O}_{sur}, \underline{a}_{sur} \right] \left[\delta_w \sin\frac{2\pi V_p t}{l_w}, 0, 0 \right]^t \tag{13}$$

Position and Orientation of the Torch

The position and the orientation of the weld torch may now be defined with respect to the frame **sur**. The orientation of the torch with respect to the frame **sur** is defined in terms of the two spherical angles β_1 and β_2. The angle β_2 rotates the torch about the weld point, whereas the angle β_1 controls the pitch of torch with respect to the part surface (see Figure 5). The stickout of the weld torch is specified as the distance to the weld surface, it is denoted by r_{stk}. The position of the tip of the weld torch can be represented by a spherical transform $\mathbf{Sph}(\beta_1,\beta_2,r_{stk})$ [6] with respect to the frame **sur**.

Kinematic Coordination of the Table

As discussed in the above the table is used to align the weld part surface normal with that of the gravity vector. If the z-axis of the frame **sur** is the surface normal then:[*]

$$
{}^{O}\mathbf{R}_{Torg} \, {}^{Torg}\mathbf{R}_{Tbl} \, {}^{Tbl}\mathbf{R}_{Part} \, {}^{Part}\mathbf{R}_{sur} = \begin{bmatrix} c_\psi & -s_\psi & 0 \\ s_\psi & c_\psi & 0 \\ 0 & 0 & 1 \end{bmatrix} = \mathbf{R}_F \tag{14}
$$

This can be clearly seen from the fact that the surface normal $a_{sur} = (0,0\ 1)^t$ has to be aligned in the direction of the gravity vector, this allows us just one degree of freedom, that is the rotation ψ about the z axis.

---

[*] Note $c_\beta = \cos(\beta)$ and $s_\beta = \sin(\beta)$

Inverse Kinematics Of The Welding Table

The joint angles of the positioning table can be obtained from the analysis of the kinematic chain: [**]

$$^{Torg}\mathbf{R}_{Tbl} = \left(^{o}\mathbf{R}_{Torg}\right)^{-1} \mathbf{R}_F \left(^{Tbl}\mathbf{R}_{Part}\,^{Part}\mathbf{R}_{sur}\right)^{-1}$$

If the matrices $\left(^{o}\mathbf{R}_{Torg}\right)^{-1} = [u_{ij}]$: $i,j = 1...3$ and,

$\left(^{Tbl}\mathbf{R}_{Part}\,^{Part}\mathbf{R}_{sur}\right)^{-1} = [q_{ij}]$: $i,j = 1...3$ and $\mathbf{R}_F = [r_{ij}]$: $i,j = 1...3$

then,
$$^{Torg}\mathbf{R}_{Tbl} = \left[\sum_{j}^{3}\sum_{i}^{3} u_i\, r_{ij}\, q_j\right] \tag{15}$$

Thus for a given table structure the joint angles and ψ can be computed from the resulting triangular equations obtained by equating terms. These equations will be of the form, $ac_\psi + bs_\psi + c = 0$, (for further discussion see example in Section V).

III. Inverse Kinematics of the Cybotech WV15 Robot and Its Singularities

The below Denavit-Hartenberg parameters define the Cybotech WV15 manipulator

---

[**] A homogeneous transform $^{A}\mathbf{T}_B = \begin{bmatrix} ^{A}\mathbf{R}_B & ^{A}\underline{P}_B \\ 0\ 0\ 0 & 1 \end{bmatrix}$, where $^{A}\mathbf{R}_B$ is a (3×3) rotation matrix relating to the orientation of frame B with respect that of frame A and $^{A}\underline{P}_B$ is the (3×1) linear displacement vector of frame B with respect to that of A.

Joint Angle	α	a	d
θ_1	90	0	$d_1 = 1000$
θ_2	0	$a_2 = 1000$	0
θ_3	-90	0	0
θ_4	90	0	$d_4 = 1000$
θ_5	-90	0	0
θ_6	0	0	0

Table 1
Robot Joint Parameters

The forward kinematics of this manipulator are obtained by concatenating the link matrices, such that

$$^B T_6 = \prod_{i=0}^{5} {}^i A_{i+1} = \begin{bmatrix} n_x & o_x & a_x & p_x \\ n_y & o_y & a_y & p_y \\ n_z & o_z & a_z & p_z \\ 0 & 0 & 0 & 1 \end{bmatrix} = \begin{bmatrix} \underset{\sim}{n} & \underset{\sim}{o} & \underset{\sim}{a} & \underset{\sim}{p} \\ 0 & 0 & 0 & 1 \end{bmatrix} \tag{16}$$

Note the symbol B is used to denote the manipulator base frame of reference. The six joint variables of the manipulator can then be solved for (we do not state all the joint solutions except those necessary for our analysis):

$$\theta_1 = \text{atan2}\,(p_y,\ p_x) \tag{17}$$

$$\theta_{23} = \text{atan2}\left\{ \left(a_2^2 - d_4^2 - \left(H_1^2 + H_2^2\right)\right),\ \left(4d_4^2\left(H_1^2 + H_2^2\right) - \left(a_2^2 - d_4^2 - H_1^2 - H_2^2\right)^2\right)^{1/2} \right\}$$

$$+ \text{atan2}\left(H_2,\ H_1\right) \tag{18}$$

where, $H_1 = c_1 p_x + s_1 p_y$, and, $H_2 = p_z - d_1$, also $H \triangleq \sqrt{(H_1^2 + H_2^2)}$. Note that in order to solve for θ_{23} we require, $4d_4^2 H^2 - \left(a_2^2 - d_4^2 - H^2\right)^2 > 0$, or

$$\left| \frac{a_2^2 - d_4^2 - H^2}{2d_4 H} \right| < 1 \tag{19}$$

The constraint posed on the solvability of θ_{23} can be clearly understood from the Figure 3. If we consider the triangle $O_2 O_3 P$, then

$$\cos A = \frac{d_4^2 + H^2 - a_2^2}{2d_4 H} = \omega \qquad (20)$$

we are therefore constrained to have $|\cos A| \leq 1$, thus if $(\omega > 1)$ then

$$H > a_2 + d_4 \qquad (21)$$

which results in the manipulator work point being out of reach.

Therefore we can conclude $H \geq a_2 + d_4$ is the θ_3 singularity state of Cybotech WV15 [1]. We desire to keep H in the interval $[0, (a_2 + d_4)]$, and for good maneuverability, we desire

$$H = C = \frac{1}{2}(a_2 + d_4) \qquad (22)$$

In this case the robot is able to stretch its arm back and forth and still avoid the singularity state of θ_3, the robot is then said to have good maneuverability.

Notice also that additional constraints exists on the solvability of θ_1 (equation (17)), thus we seek to avoid $p_x = 0$ and $p_y = 0$ simultaneouly. Equivalently we may seek to maintain

$$p_x^2 + p_y^2 \geq \delta_1 > 0 \qquad (23)$$

This corresponds to avoiding the θ_1 singularity of the WV15 manipulator, δ_1 is a small positive constant.

If θ_5 is zero then joint rotations about axis four (first wrist roll) aligns with the rotations about axis six (the final wrist roll) see Figure 3. At that time the rotation of joint four becomes colinear with the rotations of joint six. This is a singularity state, therefore we desire:

$$|\theta_5| \geq \delta_5 > 0 \quad \text{or} \quad |\cos\theta_5| \leq \delta_5' \qquad (24)$$

where the constants δ_5 and δ_5' are selected to produce desirable motion characteristics of

the wrist, see [11].

The track motion d_t should also be limited to the range $d_{tmin} \leqq d_t \leqq d_{tmax}$. If $\delta_t = |d_{tmax}| = |d_{tmin}|$, then we need $|d_t| \leqq \delta_t$.

IV. Singularity Avoidance And Coordination
of the Redundant Joints

We desire to maintain the robot close as possible to good maneuverability throughout the motion of the arm. This may be achieved through appropriate coordination of the redundant joints. We formulate this as a mathematical programming problem. The equality constraints is that:

$$^O\mathbf{T}_{track}{}^B\mathbf{T}_6 = \begin{bmatrix} ^O\mathbf{R}_w & ^O\underset{\sim}{\mathbf{P}}_w \\ 0 & 1 \end{bmatrix} \tag{25}$$

where $^O\mathbf{T}_{track}$ is the homogeneous transformation representing the track and $^B\mathbf{T}_6$ is the homogeneous transformation of the WV15 robot. The right hand side of the above equation is known and the subscript w is used to denote the workposition, and the superscript O is used to denote the workcell origin. This constraint can be subdivided further into:

$$^B\mathbf{R}_6 = (^O\mathbf{R}_{track})^t \, ^O\mathbf{R}_w \tag{26}$$

and,

$$^B\underset{\sim}{\mathbf{P}}_6 = (^O\mathbf{R}_{track})^t (^O\underset{\sim}{\mathbf{P}}_w - \,^O\underset{\sim}{\mathbf{P}}_{track}) \tag{27}$$

The transformation $^O\mathbf{T}_{track}$ consists of two transformations Z and $\mathbf{A}_0$, i.e. $^O\mathbf{T}_{track} = Z\mathbf{A}_0$,

where

$$Z = \begin{bmatrix} \mathbf{R}_z & \underset{\sim}{\mathbf{P}}_z \\ 0 & 1 \end{bmatrix} \text{ and } \mathbf{A}_0 = \begin{bmatrix} \mathbf{R}_0 & \underset{\sim}{e}_3 d_t \\ 0 & 1 \end{bmatrix} \tag{28}$$

and where constant transformations are as defined in Figure 2,

$\underset{\sim}{e}_3 = (0,0,1)^t$, $\mathbf{R}_z = \text{rot}(z,\theta_z)$, $\mathbf{R}_0 = \text{rot}(x', -\frac{\pi}{2})$, and $\underset{\sim}{\mathbf{P}}_z = \text{trans}(x',a_q)$. Note

$\mathbf{R}_z$, $\mathbf{R}_0$ and $\underset{\sim}{\mathbf{P}}_z$ can be any constant matrices. Thus we have,

$$^O\underset{\sim}{\mathbf{P}}_{\text{track}} = \underset{\sim}{\mathbf{P}}_z + \mathbf{R}_z \underset{\sim}{e}_3 d_t \tag{29}$$

and $\qquad ^B\underset{\sim}{\mathbf{P}}_6 = (\mathbf{R}_z\mathbf{R}_0)^t(^0\underset{\sim}{\mathbf{P}}_w - {}^0\underset{\sim}{\mathbf{P}}_z - \mathbf{R}_z\underset{\sim}{e}_3 d_t) = (p_x,p_y,p_z)^t \tag{30}$

A mathematical nonlinear programming model may now be constructed as follows:

$$\text{If}\quad \phi(x) = H^2 - C^2 = (p_x^2 + p_y^2 + (p_z - d_1)^2 - C^2) \tag{31}$$

then, $\qquad$ minimize $f(\underset{\sim}{x}) = \dfrac{1}{2}\,\phi(x)^2 \tag{32}$

The minimization of $f(\underset{\sim}{x})$ is designed to keep robot in good reach and avoid θ_3 singularity. The equality constraints are:

$$\underset{\sim}{h}_1(\underset{\sim}{x}) = {}^O\mathbf{T}_{\text{track}}\, {}^B\mathbf{T}_6 - \begin{bmatrix} \mathbf{R}_w & \underset{\sim}{\mathbf{P}}_w \\ 0 & 1 \end{bmatrix} = 0 \tag{33}$$

In our case this simplifies to:

$$\underset{\sim}{h}(\underset{\sim}{x}) = \begin{bmatrix} p_x \\ p_y \\ p_z \end{bmatrix} - (\mathbf{R}_z\mathbf{R}_0)^t \begin{bmatrix} {}^O\underset{\sim}{\mathbf{P}}_w - {}^O\underset{\sim}{\mathbf{P}}_z - {}^O\mathbf{R}_z\underset{\sim}{e}_3 d_t \end{bmatrix} = \begin{bmatrix} 0 \\ 0 \\ 0 \end{bmatrix} \tag{34}$$

and the inequality constraints which are designed to avoid robot singularities in θ_1 and θ_5 and maintaining the track in its workspace, is thus

$$\underset{\sim}{g}(\underset{\sim}{x}) = \begin{bmatrix} \delta_1^2 - (p_x^2 + p_y^2) \\ |\cos\theta_5| - \delta_5' \\ |d_t| - \delta_t \end{bmatrix} \leqq \begin{bmatrix} 0 \\ 0 \\ 0 \end{bmatrix} \tag{35}$$

We need to solve for $\underset{\sim}{x} = [p_x, p_y, p_z, d_t]^t$. In the above problem the equality

constraint $\underset{\sim}{h}_1(\underset{\sim}{x})$ simplifies to $\underset{\sim}{h}(\underset{\sim}{x})$ as the track is only able to alter the robot position, the orientation specified in $\mathbf{R_w}$ must be satisfied by the arm. The above problem is a standard problem of constrained minimization and a solution methodology exists and is described by the Kuhn-Tucker conditions [18]. The model we have proposed in the above *is well posed and satisfies the condition for good modelling* [23],[24].

Simplification of the Constrained Minimization
for Singularity Avoidance and Redundancy Control

As the size of our problem is quite small we may seek analytic solution from the Kuhn-Tucker conditions [18], a clearly stated approach is given in pp. 27, [24]. On examination of the Kuhn-Tucker conditions we find that the inequality constraints need only be considered when they are active, i.e. $g_j(\underset{\sim}{x}^*) = 0$, where $\underset{\sim}{x}^*$ is the optimum solution. If the inequality constraint is not violated i.e. $g_j(\underset{\sim}{x}^*) < 0$, from the complementary slackness condition [18], then the first order necessary condition (fonc) [18] only involves $f(\underset{\sim}{x})$ and $\underset{\sim}{h}(\underset{\sim}{x})$ [18] i.e.:

$$\nabla f(\underset{\sim}{x}^*) + \underset{\sim}{\lambda}^t \nabla \underset{\sim}{h}(x^*) = 0 \tag{36}$$

where $\underset{\sim}{\lambda} \in E^3$ are lagrange multipliers. Therefore a practical strategy evolves which reduces to as follows:

case(1) $\begin{cases} \text{(i)} & \text{Find solution for fonc of the equality constraint, as noted in the above.} \\ \text{(ii)} & \text{Check if the inequality constraintis violated. If not discard the inequality constraint} \end{cases}$

case(2) $\begin{cases} \text{(iii) If inequality constraint is violated revise the solution to include inequality constraint} \end{cases}$

Intuitively, if we are far from θ_1 or θ_5 singularity and $|d_t| < \delta_t$, then we may move the manipulator to maintain good maneuverability with respect to $H = C$. This is

achieved by suitable motion of the track d_t which satisfies the equality constraint. If the inequality constraints are violated, the track is moved to keep the manipulator at a safe boundary from the singularity conditions through considerations in case (2). We can now find the analytic solution for both cases:

Case(1): **Solution of the equality constraint**

This occurs when $\underset{\sim}{g}(\underset{\sim}{x}) < 0$ and in this case the after some manipulation, the fonc simplifies to:

$$\underset{\sim}{\lambda} = -4\phi(\underset{\sim}{x})[p_x, p_y, (p_z - d_1)]^T \quad \text{and} \quad \lambda^T R_0^T e_3 = 0 \tag{37}$$

leading to: $\quad$ (a) $\phi(\underset{\sim}{x}) = 0$, or (b) $\underset{\sim}{e}_3^T R_0 \begin{bmatrix} p_x \\ p_y \\ p_z - d_1 \end{bmatrix} = 0$ $\tag{38}$

This results in two solution of d_t, d_{ta} and d_{tb}:

$$d_{tb} = (\underset{\sim}{P}_w - \underset{\sim}{P}_z)^t R_z \underset{\sim}{e}_3 - R_0(3,3)d_1 \tag{39}$$

and,

$$d_{ta} = d_{tb} \pm \sqrt{d_{tb}^2 + C^2 - H_w^2 - (a_q^2 - 2a_q\sqrt{x_w^2 + y_w^2 - d_{tb}^2})} \tag{40}$$

where $H_w^2 = x_w^2 + y_w^2 + (z_w - d_1)^2$ and Δ is the term under the first square root in (40). The two solutions of the track correspond to two different regions in which they can be applied, this is clearly shown in Figure 4. There are two values of d_{ta} in the region where it is possible to satisfy, $H = C$, however when $H > C$ there is only one solution d_{tb}.

We can now analyze the second order sufficiency conditions. As, $d_{ta} = \{d_{ta} \mid f(\underset{\sim}{x}) = 0\}$ we do not consider this case further as this solution is optimum, and we only examine the second solution d_{tb}. We are required to check the positive

definiteness of the Hessian matrix[+] of $L(\underset{\sim}{x}{}^{*}) = \{\nabla f + \underset{\sim}{\lambda}\,{}^{t}\nabla\underset{\sim}{h} + \underset{\sim}{\mu}\,{}^{t}\nabla\underset{\sim}{g}\}$ on the tangent plane M:

$$M = \nabla\underset{\sim}{h} \cdot \underset{\sim}{x} = 0 \qquad (41)$$

After some manipulation this gives us[++]:

$$\begin{bmatrix} p_x \\ p_y \\ p_z \end{bmatrix} = - \begin{bmatrix} R_0(3,1) \\ R_0(3,2) \\ R_0(3,3) \end{bmatrix} d_t \quad \forall \; \underset{\sim}{x}{}^{*} \in M \qquad (42)$$

Therefore, on the tangent plane M we have $d_t^2 = p_x^2 + p_y^2 + p_z^2$. On analysis of these conditions, we find the Hessian matrix of L on the M-plane to be positive definite, this guarantees d_{tb} to be the optimum solution for $H > C$.

Case (2): Solution with the Inequality Constraint Relating to θ_1

The problem is now reformulated to:

$$\min\; f(\underset{\sim}{x}) \mid \underset{\sim}{h}\,(\underset{\sim}{x}) = 0 \; ; \; g_1(\underset{\sim}{x}) = \delta_1^2 - (p_x^2 + p_y^2) \leqq 0 \qquad (43)$$

The feasible solution set is formed by $\underset{\sim}{h}\,(\underset{\sim}{x}) = 0$ and $g_1(\underset{\sim}{x}) = 0$. Note that $\underset{\sim}{h}\,(\underset{\sim}{x})$ is an equation of a line and $g_1(\underset{\sim}{x})$ is that of a cylinder, this leads to at most two solutions of $\underset{\sim}{x}$ in which case the solution of $\underset{\sim}{h}\,(\underset{\sim}{x}) = 0$ is:

$$\begin{bmatrix} p_x \\ p_y \\ p_z \end{bmatrix} = \begin{bmatrix} \alpha_x + \beta_x d_t \\ \alpha_y + \beta_y d_t \\ \alpha_z + \beta_z d_t \end{bmatrix} \qquad (44)$$

[+]Note $\underset{\sim}{\mu} = \underset{\sim}{0}$ in case(1), as constraints are inactive.

[++]$R_0(3,1) \equiv (3,1)$ component of R_0 matrix.

where $\underset{\sim}{\alpha} = -(R_z R_0)^t (\underset{\sim}{P}_w - \underset{\sim}{P}_z)$ and $\underset{\sim}{\beta} = [R_0(3,1), R_0(3,2), R_0(3,3)]^t$ (45)

Note also $g_1(\underset{\sim}{x}) = 0$, leads us to :

$$p_x^2 + p_y^2 = \delta_1^2 \qquad (46)$$

Therefore d_t can have at most two possible solutions,

$$d_t = \frac{-(\alpha_x \beta_x + \alpha_y \beta_y) \pm \sqrt{(\alpha_x \beta_x + \alpha_y \beta_y)^2 - (\beta_x^2 + \beta_y^2)(\alpha_x^2 + \alpha_y^2 - \delta_1^2)}}{(\beta_x^2 + \beta_y^2)} \qquad (47)$$

The feasible region can at most only contain two points and we need to choose a value of d_t which makes the objective function $f(\underset{\sim}{x})$ the smallest.

Case (2): Inequality Constraint Related to θ_5

In the appendix of this paper we have shown that $\cos\theta_5$ of the Cybotech WV15 manipulator may be represented directly interms of cartesian parameters of its end effector as:

$$\cos\theta_5 = \left\{ \frac{\varsigma_1 \eta_{23} - a_z \varsigma_{23}}{2 d_4 H^2 H_1} \right\} \qquad (48)$$

where ς_1, ς_{23}, η_{23}, H and H_1 are all functions of cartesian coordinates of the end effector (see appendix). The variable ς_1 is dependent on the orientation of the end effector and all other variables in θ_5 is dependent on p_x, p_y, p_z. If the θ_5 inequality constraints becomes active the optimization problem now becomes:

$$\min f(\underset{\sim}{x}) \mid \underset{\sim}{h}(\underset{\sim}{x}) = 0 ; \; g_2(\underset{\sim}{x}) = |\cos\theta_5| - \delta_5' \leqq 0 \qquad (49)$$

Here we are required to solve a set of nonlinear equations $\underset{\sim}{h}(\underset{\sim}{x}) = 0$, in order $g_2(\underset{\sim}{x}) = 0$, to find feasible regions of d_t. After substitution one nonlinear equation will remain. The solution to this may than be found by Brent's algorithm [+] or Fibonacci

---

[+] Brents algorithm finds the zero of a function, such that the function changes sign in a given interval [25].

search or Golden search [18]. As our algorithm is called by the trajectory generator every sample time, it turns out that small displacements in d_t are usually produced to satisfy $g_2(\underset{\sim}{x})$ inequality.

Inequality Constraint Related to d_t

If $g_3(\underset{\sim}{x})$ constraint is violated, then a d_t value is selected which makes $\underset{\sim}{h} (\underset{\sim}{x}) = 0$, simultaneously with $g_3(\underset{\sim}{x}) = |d_t| - \delta_t \leq 0$. Satisfying $g_3(\underset{\sim}{x})$ involves the resetting d_t to its joint limits. This solution is possible in the range, $\delta'_1 \leq H \leq a_2 + d_4$, outside of which the manipulator and track is unable to reach the workpoint $\underset{\sim}{P}_w$. Offline global planning must ensure such out of reach conditions do not occur.

Computer Implementation of the Algorithm
and Computational Issues

The implementation of the algorithm to coordinate the track and robot is now described by the following practical strategy. The algorithm is called by the trajectory generator once every trajectory sample time, once the weld point on the part is calculated in the trajectory.

Step 1:   Find $^OT_w(t) = \begin{bmatrix} R_w & \underset{\sim}{P}_w \\ 0 & 1 \end{bmatrix}$ from trajectory calculations.

Step 2:   Find appropriate d_t which minimizes $f(\underset{\sim}{x})$ and maintains equality constraints, possible solutions are d_{tb} (equation (39)) and $d_{ta} = d_{tb} \pm \sqrt{\Delta}$, where Δ is as shown in equation (40).

Then select d_t as follows:

$$\text{Stage (1)} \quad d_t' = \begin{cases} d_{ta} & \text{if } \Delta \geqq 0 \\ d_{tb} & \text{if } \Delta < 0 \end{cases}$$

$$\text{Stage (2)} \quad d_t = \begin{cases} d_{tmin} & \text{if } d_t' < d_{tmin} \\ d_t' & \text{if } d_{tmin} \leqq d_t' \leqq d_{tmax} \\ d_{tmax} & \text{if } d_{tmax} < d_t' \end{cases}$$

Step 3: Find $\underset{\sim}{p}$ and $\underset{\sim}{a}$, (see equation (16)) from equation (30) i.e. $\underset{\sim}{h}(\underset{\sim}{x}) = 0$ and

$$\underset{\sim}{a} = (R_z \ R_o)^T R_w \underset{\sim}{e}_3$$

Step 4: Check if singularity of θ_1 is avoided (equation (23)), if not select new d_t from equation (47) minimizing $f(\underset{\sim}{x})$.

Step 5: Check if singularity of θ_5 is avoided using equation (49), if not select a new d_t which satisfies (49) using Fibonacci or Brents algorithm.

Step 6: If new d_t in step 5 go back to step 3.

Step 7: Calculate $^B T_6 = {}^O T_{track}^{-1} \begin{bmatrix} {}^O R_w & {}^O \underset{\sim}{P}_w \\ 0 & 1 \end{bmatrix}$ and solve for $\theta_i \mid i = 1...6$.

Step 8: Stop

Computational Issues

The number of mathematical operations involved in each step is given as per below.

Step 1: 73m + 38a + 4f

Step 2: 15m + 15a + 1 sqrt

Step 3: 24m + 18a

Step 4: 8m + 6a + 1 sqrt

Step 5: 25m + 11a + 1 sqrt + 1 div

Step 6: (57m + 35a + 2 sqrt + 1 div) * k

Step 7: 9m + 6a

where 'm' denotes multiplication, 'a' denotes addition and 'sqrt' denotes square root and 'f' denotes transcendental function call and 'div' denotes division. We note in Step 6 'k' represents the number of iterations of Step 3, 4 and 5 needed to find a suitable d_t void of singularities, usually k=5. Therefore total time needed to obtain the joint solutions is greater than 439m + 269a + 10 sqrt + 4f + 6 div. For a Motorola 16MHZ 68020 + 68881 microprocessor set this represents a minimum computation time of 439 (5.87) + 269 (4.66) + 10 (7.9) + 4(28.47) + 6 (7.78) $\cong$ 4 ms. The actual implementation time would greatly depend on the system software organization.

V. Simulation of Welding Operation
with a Redundant Manipulator

The purpose of this simulation is to verify the proposed redundancy and coordination control scheme can be used in complex welding applications. We have assumed the following problem:

1)   The part is mounted on a two axis Pitch-Roll table, ^{Torg}Tbl with the following parameters:

θ	α	a	d
$\theta_1 = 0$	$-\pi/2$	0	0
$\theta_2 = $ var.	$+\pi/2$	0	0
$\theta_3 = $ var.	0	0	0

where θ_1 is permanently zero, and θ_2 and θ_3 are variable.

2)   The part to be welded is a skewed pipe (see Figure 6) with the surface given by

$$\text{surf}(r, \alpha, z) = r - \frac{1}{100^2}(z - 1000)^2 - 100 = 0 \tag{51}$$

3)   The part is positioned such that it is offset from the axis of rotation of both joints of the table, and down-handed welding is used. The weld tool is as shown in Figure 6.

4)   The weld path is a spiral on the surface of the skewed pipe. The equation of the path is

$$r = \text{rcurv}(\lambda) = \frac{1}{100^2}(\lambda - 1000)^2 + 100 \tag{52}$$

$$\alpha = \alpha\text{curve}(\lambda) = k\lambda \quad ; \quad z = z\text{curve}(\lambda) = \lambda \tag{53}$$

where $z \in [0, 2000]$ and in the range $\alpha \in [0, 2\pi]$, the pitch of the spiral is given by $k = 2\pi/2000$.

6)   The welding speed $\dfrac{ds}{dt}$ is constant i.e. velocity of the tip of the torch relative to the path on the part is constant, therefore $\dfrac{ds}{dt} = \left(\sqrt{dr^2 + r^2 d\alpha^2 + dz^2}\right)/dt = \text{constant}$. In this simulation trajectory sample points are taken from the equally divided segments along the length of the weld curve. The length of the weld curve s is given as:

$$s = \int \sqrt{dr^2 + r^2 d\alpha^2 + dz^2} = \int_0^{2000} \left[\sqrt{[\frac{d\text{rcurv}(\lambda)}{d\lambda}]^2 + k^2 + 1}\right] d\lambda \tag{54}$$

8)   The Torch is tilted at an angle β_1 with the normal of the part surface and is oriented along the line tangential to the path, such that the related transform is (see Figure 5) $\text{Rot}(x, -\beta_1)$.

The necessary kinematic equations for the table is given in Section II, and ψ (the orientation of the weld trajectory) can be determined. We can determine $^{Torg}R_{Tbl}$ in Eq. (14), therefore the joint variables of the table can be computed as

$$\theta_2 = atan2(^{Torg}R_{Tbl_{13}}, - {}^{Torg}R_{Tbl_{23}}), \quad \theta_3 = atan2(^{Torg}R_{Tbl_{31}}, {}^{Torg}R_{Tbl_{32}}) \quad (55)$$

9) The track has two adjustable parameters a_q and θ_z (as shown in Figure 2), then the optimal position of track for equality constraint following the discussion of the previous section is:

$$d_{tb} = -x_w\sin\theta_z + y_w\cos\theta_z . \quad (56)$$

Notice that d_{tb} is independent of a_q. Then d_{ta} is given as:

$$d_{ta} = d_{tb} \pm \sqrt{d_{tb}^2 + C^2 - H_w^2 - a_q^2 + 2a_q(y_w\cos\theta_z + y_w\sin\theta_z)} \quad (57)$$

Obviously, if $d_t = d_{ta}$ then $H^2 = C^2$, and the track is moved to keep the robot in good maneuverability, $C = \dfrac{1}{2}(a_2 + d_4)$, then robot joint θ_3 is always maintained at $30°$. If $d_t = d_{tb}$, the track is moved such that the distance from point $\underset{\sim}{P}_w$ to the track is the shortest, so as to prevent the "out of reach" condition. The explanation of this phenomena is easily seen from Figure 4. Characteristic of this state is $\theta_1 = 0°$ or $180°$. In the singularity state of θ_1, d_t is determined by:

$$d_{t1} = x_w\sin\theta_z - y_w\cos\theta_z \pm \sqrt{\delta_1^2 - (x_w\cos\theta_z - y_w\sin\theta_z)^2} \quad (58)$$

The results of the simulation are shown in Figures 7 through 11, and are discussed below.

Analysis of Simulation Results

The organization of the robot welding system is shown in Figure 2, the projection of the weld trajectory on the XY plane of the world coordinate frame is shown in Figure 7. Start of the weld location is at the topmost corner of Figure 7, $(X, Y)^t = (0.4, 6.8)^t$. The end of weld trajectory is located at (-1, -7.4). The YZ view of the weld trajectory is also shown in Figure 7, notice there is only a small change in the Z position of the weld seam. The tool direction ψ is shown in Figure 8. The angular motions of table are also shown in the Figure 8. Note that $180° = -180°$ for table θ_2 and there is no discontinuity in the table motions.

Figure 9, shows the motions of the track along the weld path. For $d_t > 0$, H = C, is satisfied and the track and robot joint #1 is moved to achieve H = C. For the weld length s, $1.02 \leq s < 1.53$, notice that when H > C, the d_{tb} solution is used to move the track. Also note in this region robot joint #1 is not moved, see Figure 9. For $s \geq 1.53$, H = C is satisfied then d_{ta} solution is used and joint #1 is again moved.

In the above simulation θ_1 and θ_5 inequality constraints were not violated. Therefore the motions of the track is produced to satisfy only the equality constraints. Motion of the joints #2 and #3 are small as the z position of the weld trajectory is more or less constant over the entire trajectory. In order to address the issue of singularity avoidance, another weld trajectory is generated such that a θ_5 singularity is generated (see Figures 10). From the simulations shown in Figures 10, it is seen that appreciable joint motions occur in θ_4 and θ_6, as θ_5 approaches its singularity; this is undesirable. If, however, the track is moved to avoid θ_5 singularity by activating θ_5 inequality constraint, then θ_5 is maintained at a distant $\cos^{-1}(\delta_5')$ (Figure 11) from its singularity configurations. The range of motions the joints θ_4 (Figure 11) and θ_6 (Figure 11) execute is now much smaller as the trajectory passes through this neighborhood of planned θ_5 singularity.

Continuity of Joint Motions

The trajectory generated by the constrained minimization while avoiding singular configurations may generate large joint or track excursions for short periods as the inequality constraints are activated.

To remedy this several possibilities exists:

(a) Two limits of the inequality constraint activity may be adopted: (i) a soft limit (ii) a hard limit. If the system is outside the soft limit the inequality is discarded. If it is inside both limits, a solution is generated which repels the manipulator from this region. The closer the manipulator gets to the hard limit, the stronger the repelling force. The number of limits may be further discretized with a weighting placed on each level, the highest penalty being placed on the innermost limit.

Although this may generate solutions which will produce slightly smaller excursions of the track and joint motions near regions where the inequality constraints become active. It does not guarantee a solution which can be executed by the manipulator. Global off line planning is necessary to guarantee smooth motion demands. This can be produced by this algorithm if the planned trajectory is far from θ_1, θ_5 and d_t inequality constraints. This obviously requires the optimal placement of the welding table and the track with respect to the robot.

(b) In order to guarantee the trajectory generated by this scheme is executable by the manipulator. The torque and velocity constraints need to be considered in which case the exact manipulator and track dynamics is needed (this is hardly ever the known!) with the required trajectory initial conditions. Therefore in order to guarantee trajectory realization off-line, global planning would be required, such algorithms have been developed for nonredundant arms [13], [14], [15], [16]. The weld velocity (ds/dt) may be reduced to produce the desired motions qualities,

this is known as trajectory scaling and it has been studied for nonredundant arms [16]. Khatib [19] has addressed the control of the redundant manipulator through singular configurations in so called "operational space", the coordinates of the task frame, but he has not addressed the problems relating to torque saturation. Some issues related to this problem has been addressed in [20].

(c)   On the practical side, an industrial manipulator such as the cybotech WV15 on a track has large inertia with mechanical time constants of several hundred milliseconds. Trajectory profiles such as these generated by our simulation would be smoothed out by the feedback controller as perfect trajectory tracking may not be expected. As a result during implementation we can expect acceptable robot behavior.

VI. Conclusions

In this paper we have presented an algorithm to coordinate a welding table and a seven degree of freedom manipulator. The motions of the table are constrained by the down hand welding. The motions of the redundant manipulator is selected from a cartesian coordinate nonlinear optimization process to avoid robot singularities and track motion limits. This algorithm did not utilize generalized jacobian inverses like previously proposed schemes [4], [5], [9], [12], [17], [21], [22]. The desired motion accuracies have been achieved by utilizing inverse kinematics. We have been able to carry out the optimization in cartesian space because we were able to express the manipulator singularity conditions in terms of the cartesian coordinates of the end effector. Our simulation results show global offline planning of the manipulator trajectory is necessary for the placement of the welding table and the track with respect to the robot in order to ensure smooth joint motions of the track and robot.

Acknowledgements

References

[1] Ahmad, S., Luo, S., "Analysis of Kinematic Singularaties for Robot Manipulators in Cartesian Coordinate Parameters," Proceedings of the 1988 IEEE Robotics and Automation Conference, Philadelphia, PA, April 24-29.

[2] Chang, P.H., "A closed-form solution for the control of manipulators with kinematic redundancy," 1986 IEEE Intl. Conf. on Robotics & Automation, p. 9.

[3] Freund, E., Hoyer, H., "Collision avoidance in multi-robot systems," Robotics Research: 2nd International Symposium 1985, Ch. 3, pp. 135-146.

[4] Klein, C.A., Huang, C.H., "Review of pseudo inverse control for use with kinematically redundant manipulators," IEEE V. SMC-13, p. 245.

[5] Liegeois, A., "Automatic supervisory control of the configuration and behavior of multibody mechanisms," IEEE V. SMC-7, p. 868.

[6] Paul, R.P., "Robot manipulators: Mathematics, Programming, and Control," Cambridge: MIT Press, 1981.

[7] Paul, R.P., Renaud, Stevenson, C., "A systematic approach for obtaining the kinematics of recursive manipulator based on homogeneous transformations," Robotics Research: International Symposium, 1984.

[8] Tsai, L.W., Morgan, A.P., "Solving the kinematics of the most general six- and five-degree-of-freedom manipulators by continuation method," J. of Mechanism, Transmissions, and Automation in Design, June 1985, Vol. 107, pp. 189-200.

[9] Yoshikawa, T., "Analysis and control of robot manipulators with redundancy," Robotics Research: International Symposium, 1984.

[10] Zheng, Y.F., Luh, J.Y.S., "Control of two coordinated robots in motion," Proc. 24th IEEE Conf. on Decision and Control, Florida.

[11] Stevenson, C., Paul, R.P., "Kinematics of Robot Wrists," Int. J. of Robotics Research, Vol. 2, No. 3, 1983, pp. 31-38.

[12] Whitney, D.E., "Resolved motion rate control of manipulators and human protheses," IEEE Transactions on Man-Machine Systems MMS-10, 1969, pp. 47-53.

[13] Bobrow, J.E., "Optimal control of robotic manipulators," Ph.D. Thesis, University of California, Los Angles, CA, Dec. 1982.

[14] Bobrow, J.E., Gibson, J.S., Dubowsky, S., "On the optimal control of robotic manipulators with actuator constraints," Proc. 1983 American Controls Conference, San Francisco, June 1983, pp. 782-787.

[15] Shin, K.G., McKay, W.D., "Minimum-time control of robotic manipulators with geometric path constraints," IEEE Transactions on Automatic Control, Vol. AC-30, No. 6, June 1985.

[16] Hollerbach, J.M., "Dynamic scaling of manipulator trajectories," ASME Journal of Dynamic Systems, Measurement and Control, March 84, pp. 102-106.

[17] Nakamura, Y., Hanufusa, H., "Inverse kinematic solutions with singularity robustness for robot manipulator control," ASME Journal of Dynamic Systems Measurement and Control, September 1986, Vol. 198, pp. 163-171.

[18] Luenberger, D.G., "Linear and Nonlinear Programming," Addison Wesley, Menlo Park, California, 1984.

[19] Khatib, O., "A Unified Approach for Motion and Force Control of Robot Manipulators: The Operational Space Formulation," IEEE Journal of Robotics and Automation, Vol. RA3, February 1987, pp. 43-54.

[20] Hollerbach, J.M., Suh, K.C., "Redundancy Resolution of Manipulators through Torque Optimization," Proceeding of the 1985 IEEE Conference on Robotics and Automation, St. Louis, MO, pp. 1016-1021.

[21] Luh, J.Y.S., Gu, Y.L., "Industrial Robots with Seven Joints," Proceedings of the IEEE Conference on Robotics and Automation, St. Louis, MO, pp. 1010-1015.

[22] Fisher, W.D., "The Kinematic Control of Redundant Manipulators," Ph.D. Thesis, Purdue University, Aug. 1984.

[23] Berkovitz, L.D., "Lectures in Optimization," Purdue University, School of Mathematics.

[24] Vicent, T.L., Grantham, W. J., "Optimality in Parametric Systems," John Wiley 1981.

[25] IMSL Libarary manuel, 10th edition.

[26] Ahmad, S., Guo H., "Dynamic Coordination of Dual-Arm Robotic Systems," Proceedings of the 1988 IEEE Robotics and Automation Conference, April 24-29, Philadelphia, PA.

Appendix

Representation of $\cos\theta_5$ in

Cartesian Coordinate Parameters

If $^BT_6$ is as given in equation (22). Then $\cos\theta_5$ can be expressed as:

$$\cos\theta_5 = \frac{-\xi_1\eta_{23} + a_z\xi_{23}H_1}{2d_4H_1H^2}$$

where:

$$H_1 = \mathrm{sgn}_1 \sqrt{p_x^2 + p_y^2} \qquad \mathrm{sgn}_1 = \begin{cases} +1 \text{ ; shoulder up} \\ -1 \text{ ; shoulder down} \end{cases}$$

$$H_2 = p_z - d_1$$

$$H^2 = H_1^2 + H_2^2$$

$$\xi_1 = p_x a_x + p_y a_y$$

$$\eta_1 = p_x a_y - a_x p_y$$

$$\xi_D = H^2 + d_4^2 - a_2^2$$

$$\eta_D = \mathrm{sgn}_3 \sqrt{(4d_4^2 H - \xi_D^2)} \qquad \mathrm{sgn}_3 = \begin{cases} +1 \text{ ; elbow up} \\ -1 \text{ ; elbow down} \end{cases}$$

$$\xi_{23} = H_1\eta_D + H_2\xi_D$$

$$\eta_{23} = H_2\eta_D - H_1\xi_D$$

LIST OF FIGURES

CAD data

path
generation

x

coordinator

global constraints

local
constraints

nonlinear
optimization

x1   x2

table
inverse
kinematics

robot 1 | robot 2

inverse kinematics

table
control

robot 1 | robot 2

controller

Figure 1:
Hierarchical coordination of multiple
robotic devices for welding
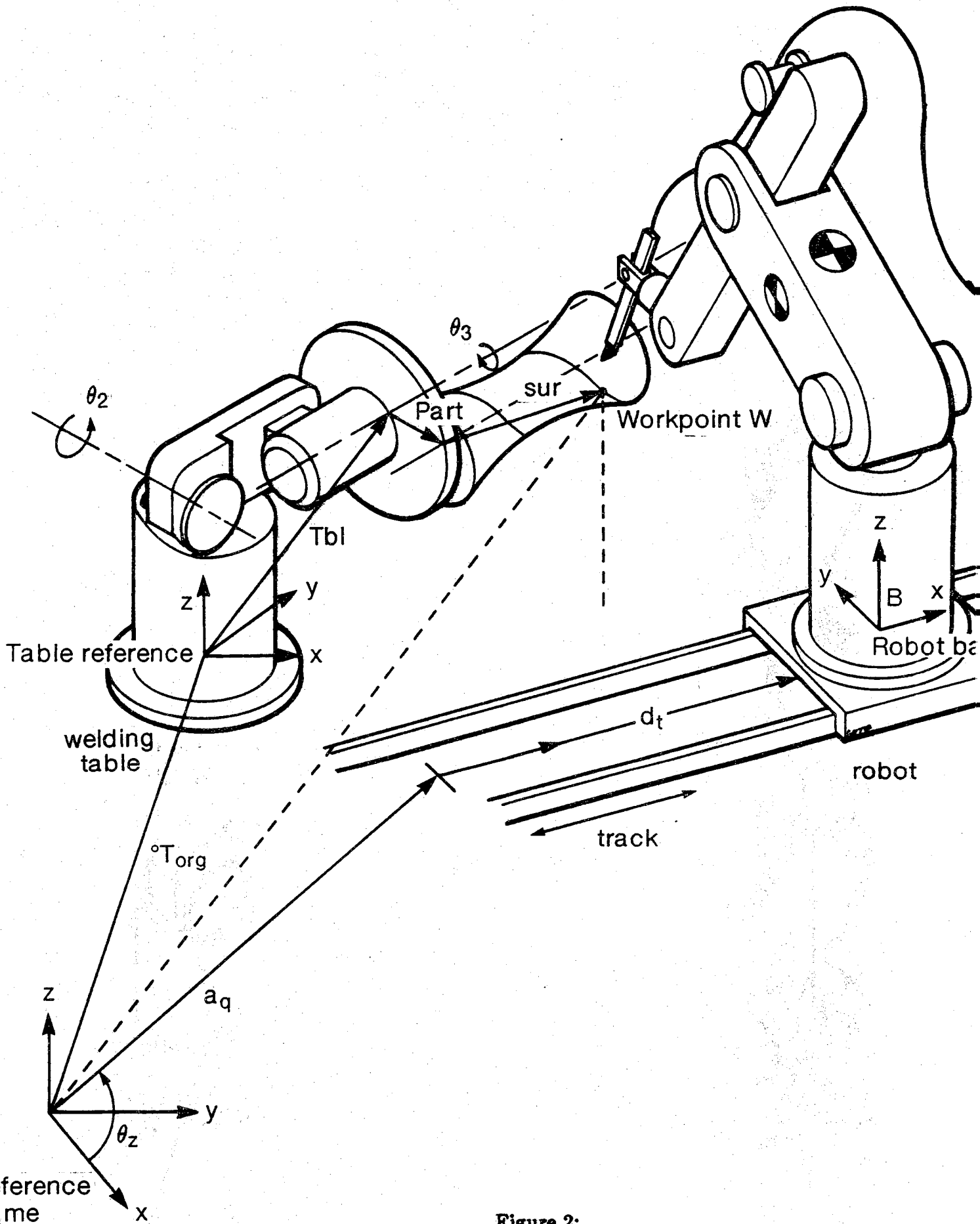
Figure 2:
Organization of the robot welding system
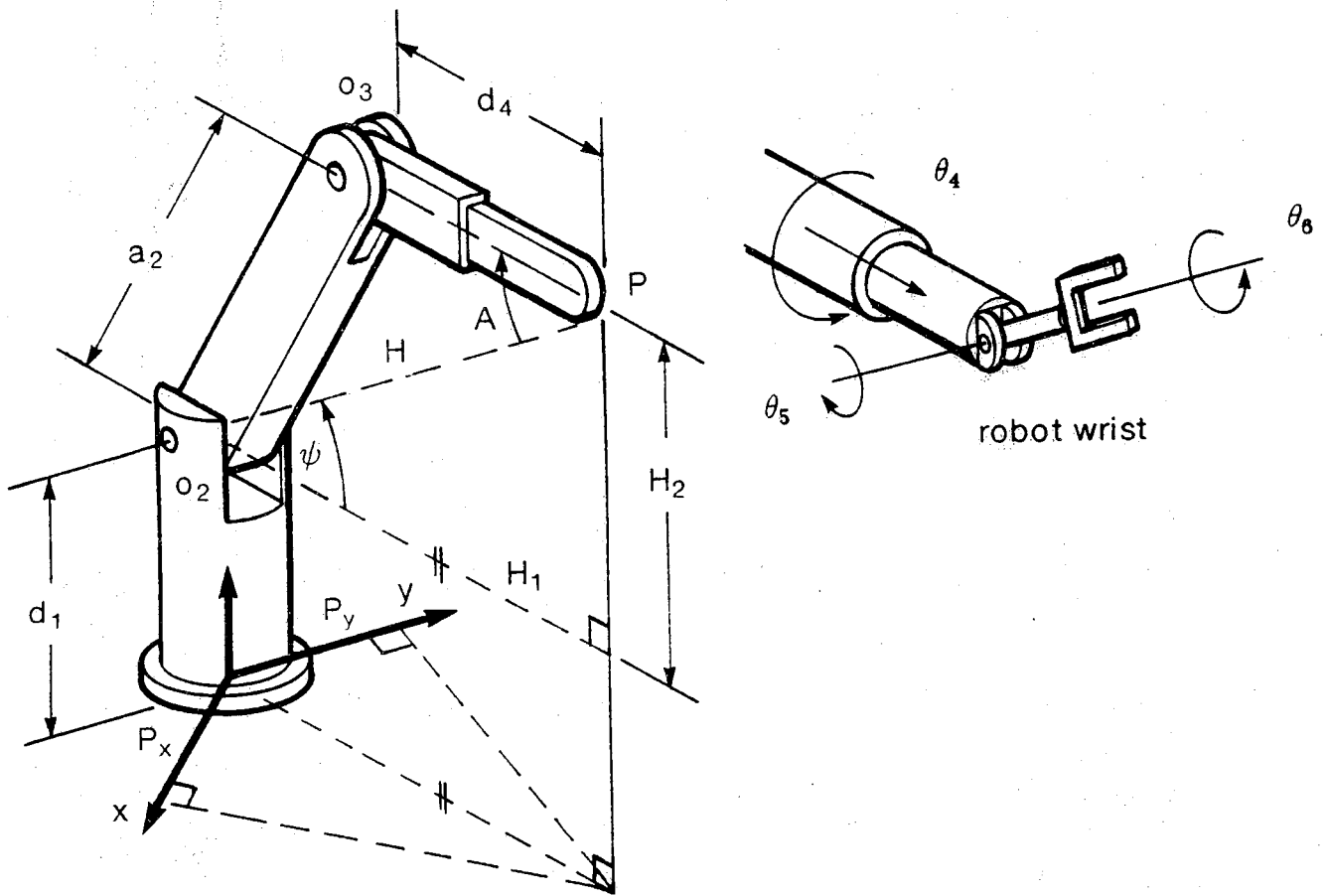
Figure 3:
Cybotech WV15, singularities of θ_3, θ_5
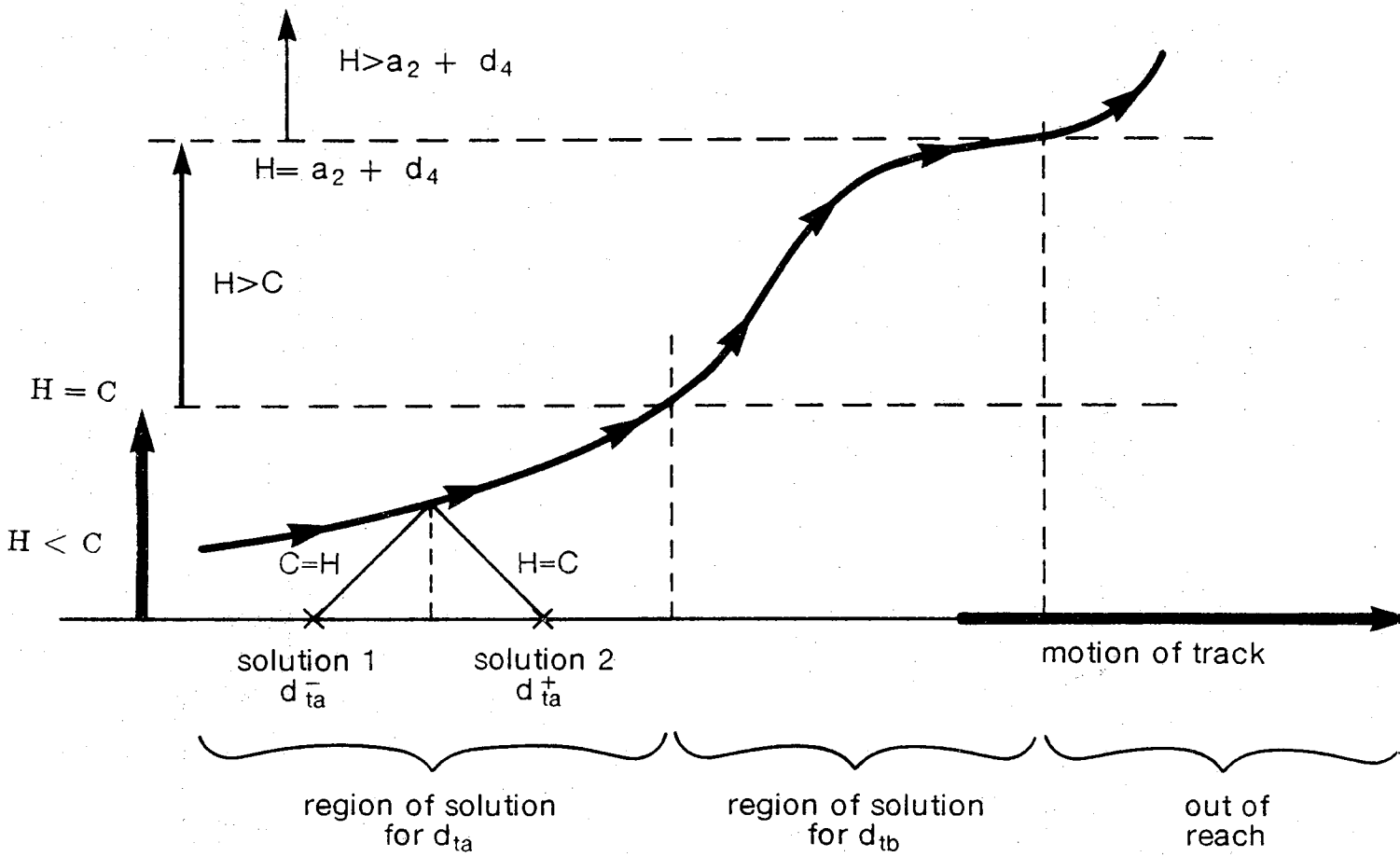
Figure 4:
Regions of solution of the track d_t
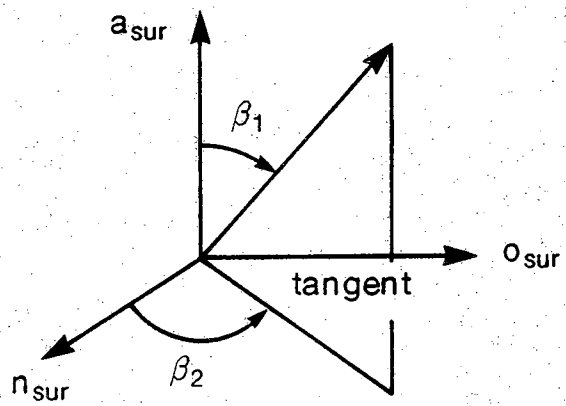
Figure 5:
Weld piece and weld tool

$$d_6 = 100$$

$$a_7 = 10$$

$$d_7 = 100$$
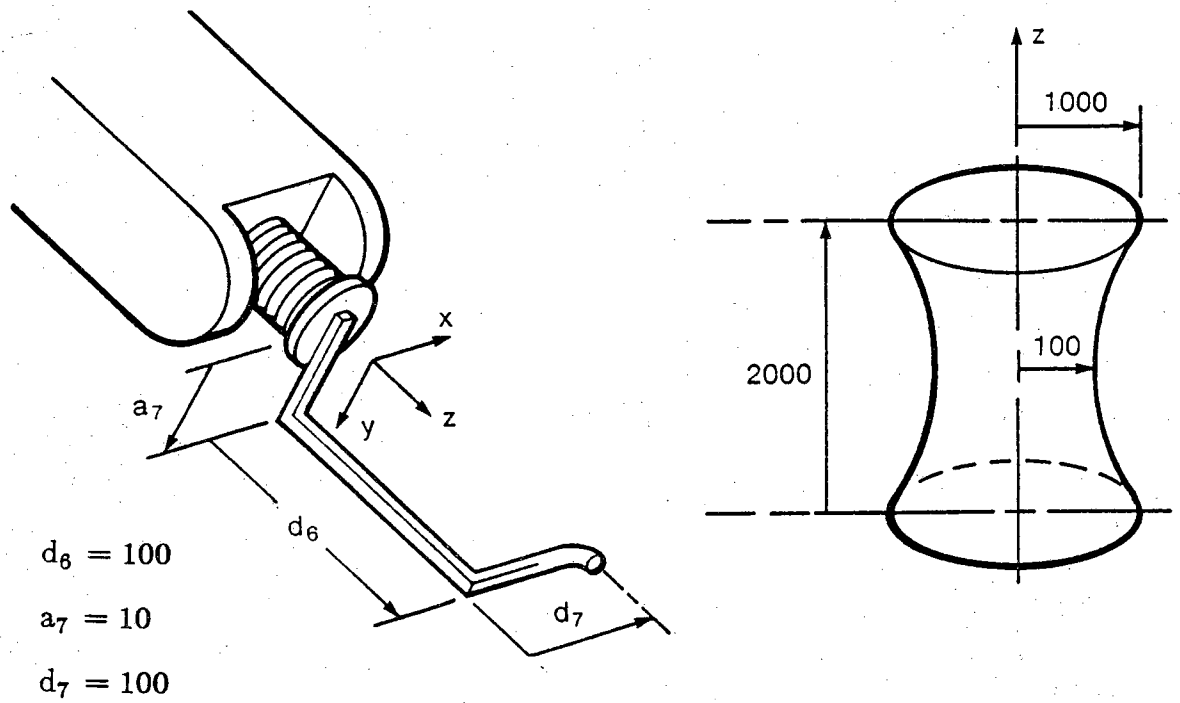
Figure 6:
Weld torch orientation
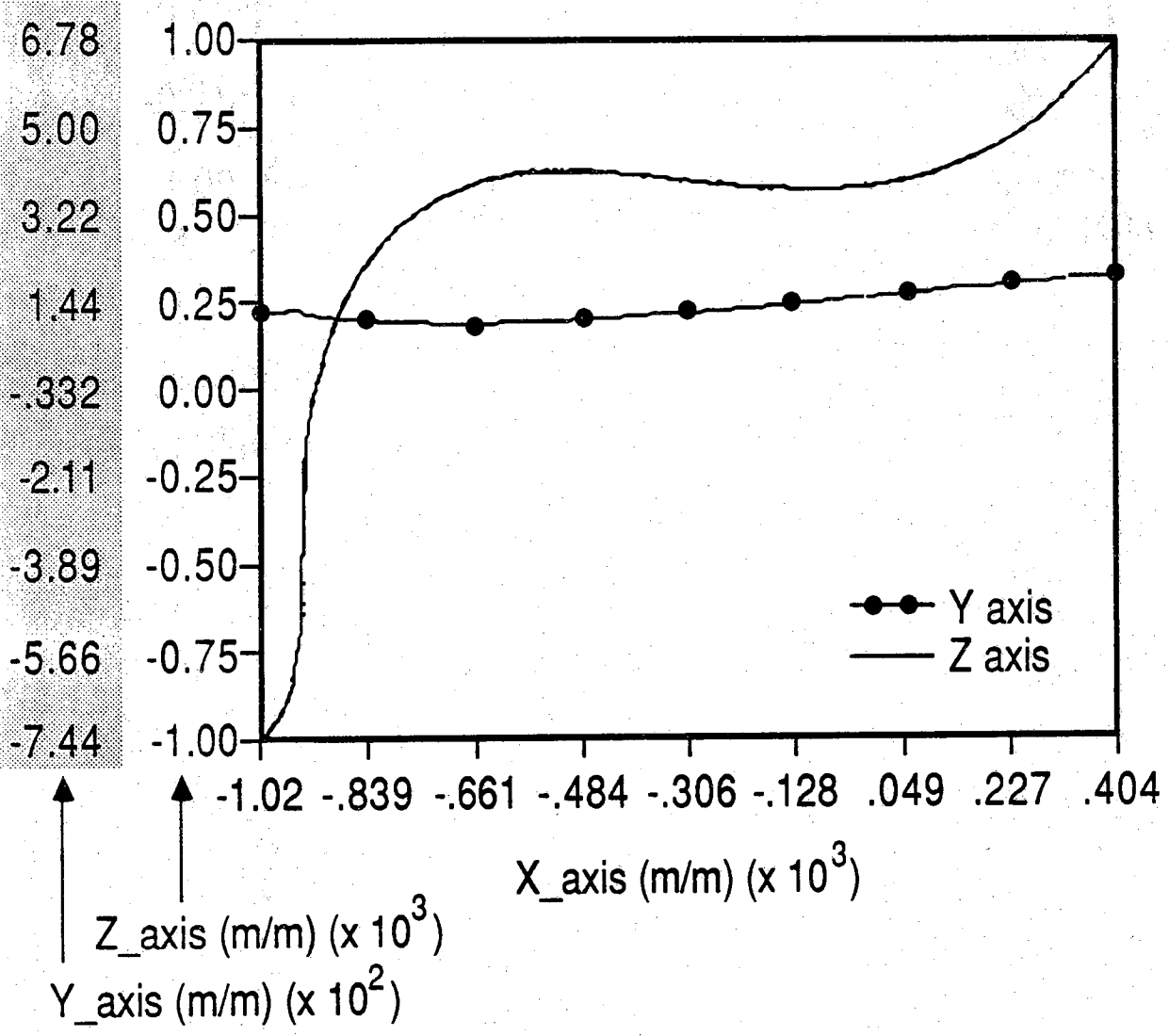
Figure 7:
World View of Weld Trajectory
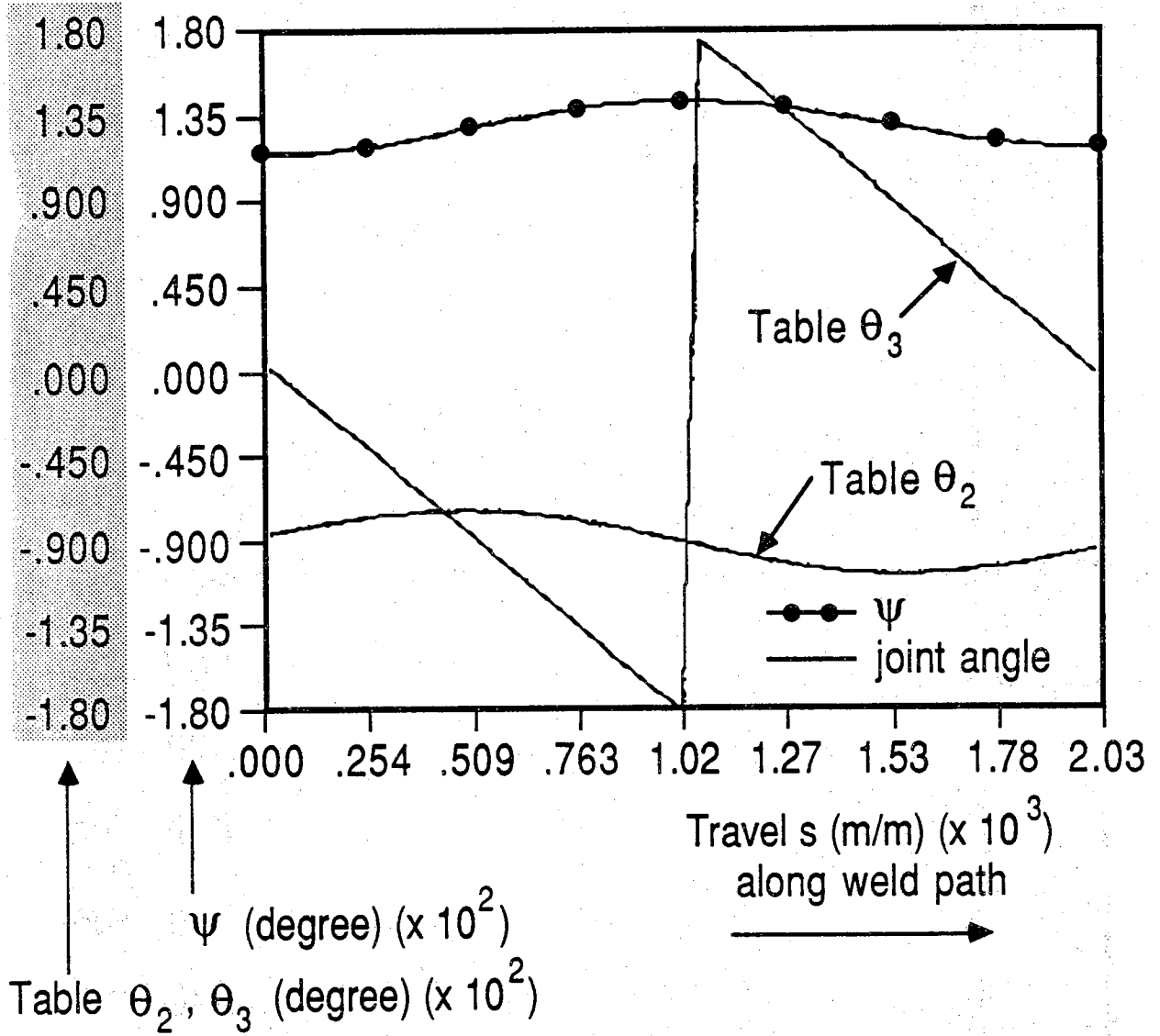
Figure 8:
Table Solutions and Weld Direction

Figure 9:
Track and Joint Solutions
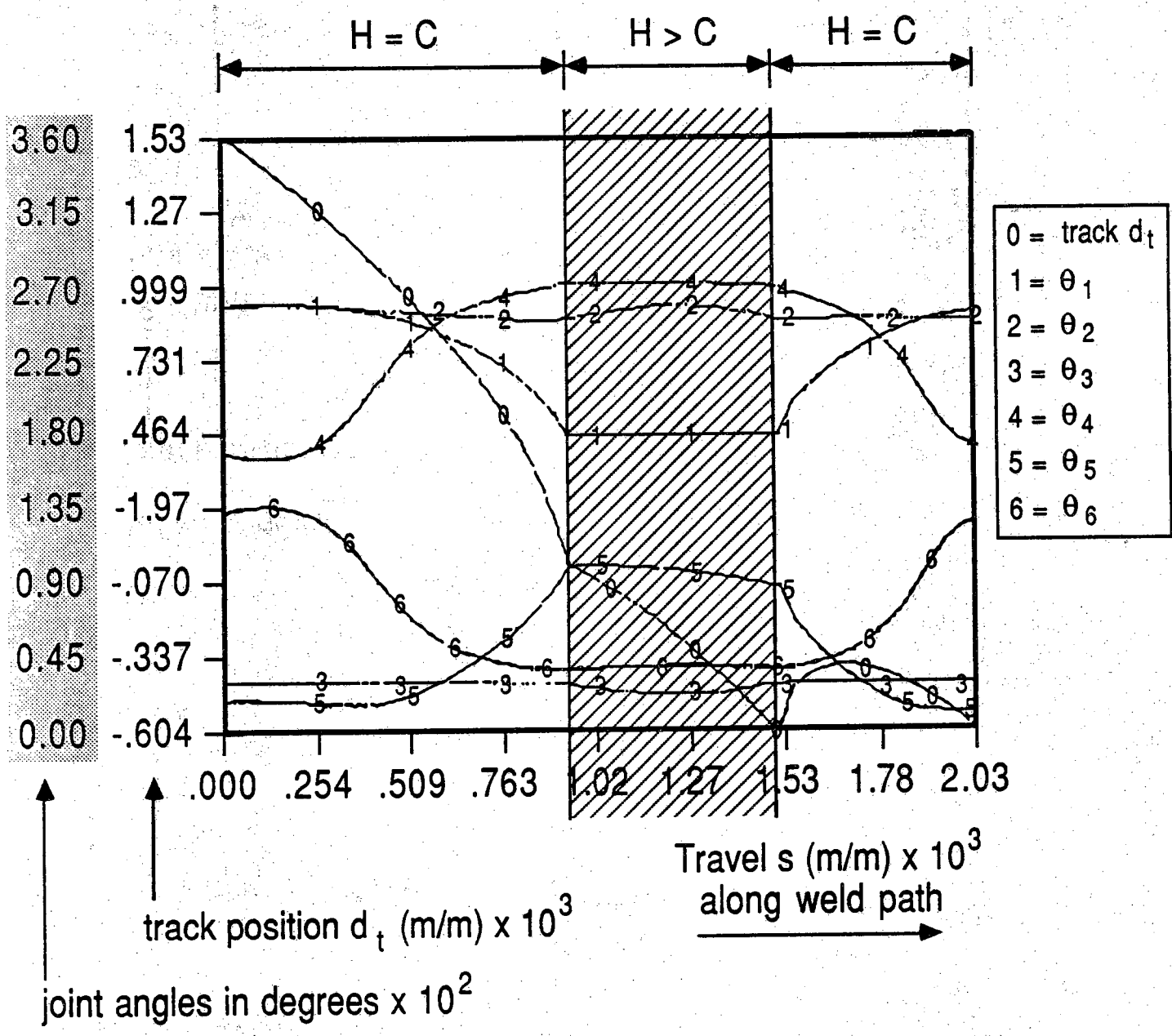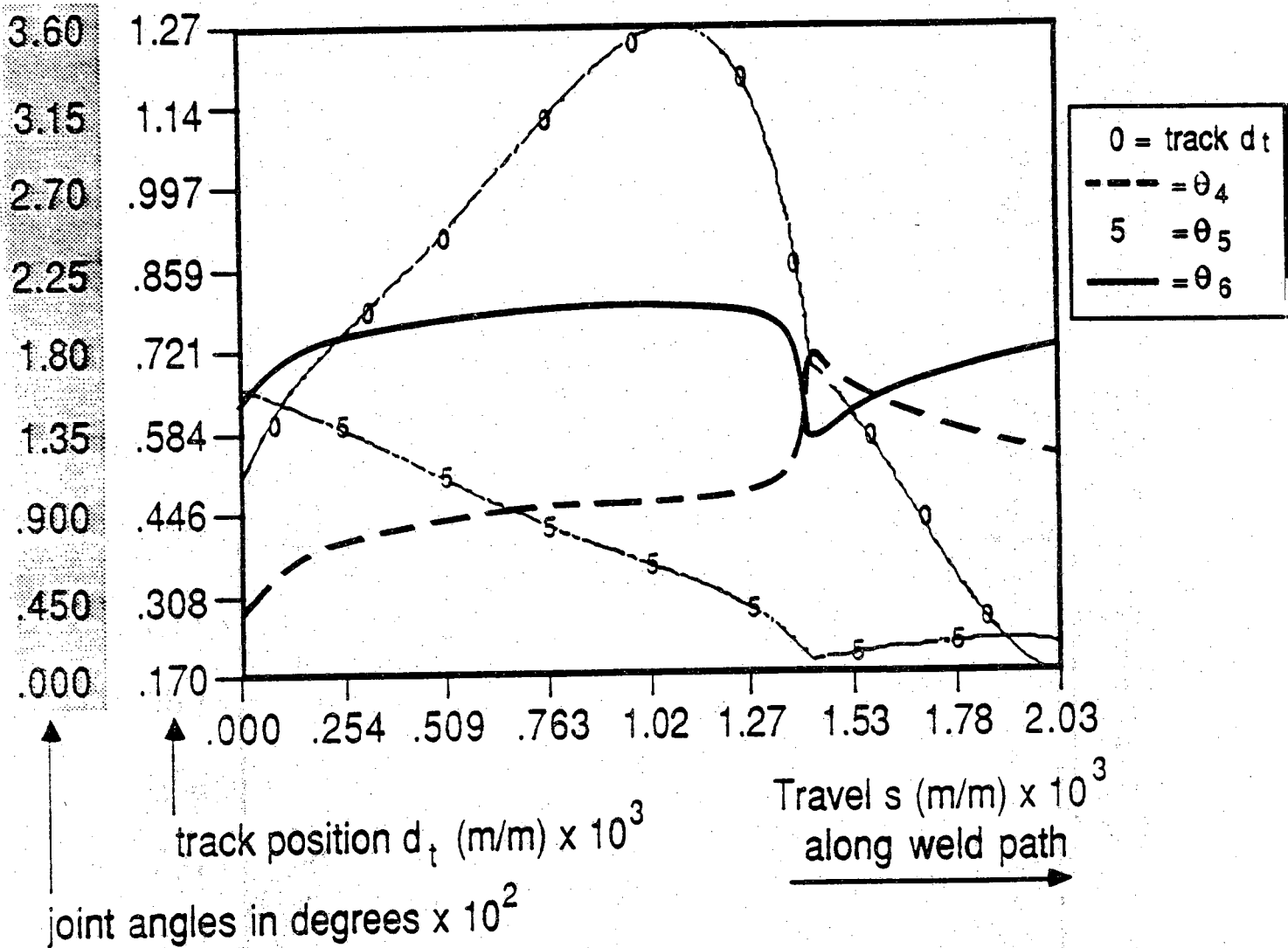
Figure 10:
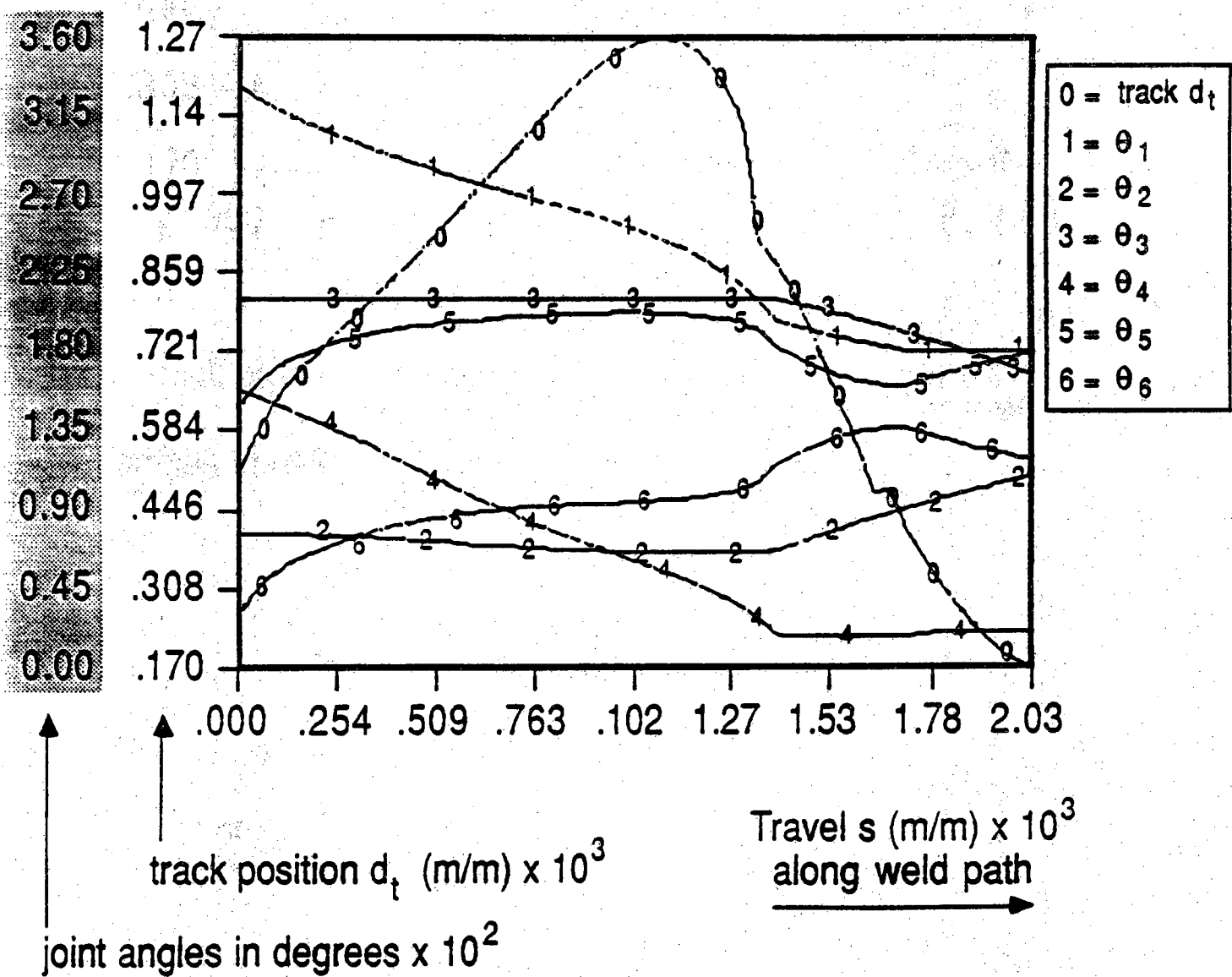Track and Joint Solutions with θ_5 Singularity

Figure 11:
Track and Joint Solutions Avoiding θ_5 Singularity